Available online at www.sciencedirect.com
SCIENCE DIRECT®
Microporous and Mesoporous Materials 74 (2004) 171–178
MICROPOROUS AND MESOPOROUS MATERIALS
www.elsevier.com/locate/micromeso

Synthesis of ZSM-5 zeolite in fluoride media: an innovative approach to tailor both crystal size and acidity

Benoît Louis *, Lioubov Kiwi-Minsker

Laboratory of Chemical Reaction Engineering, Swiss Federal Institute of Technology, LGRC-EPFL, CH-1015 Lausanne, Switzerland

Received 19 December 2003; received in revised form 17 June 2004; accepted 21 June 2004

Abstract

ZSM-5 zeolites were prepared at neutral pH by fluoride-mediated synthesis. The degree of crystallinity, the specific surface area and the crystal size are higher than those of the zeolites prepared under alkaline conditions. Moreover, by varying the F/Si ratio from 0.3 to 1.6, the H–[F]–ZSM-5 zeolites with crystal size ranging from 10 to 75 μm and the specific surface areas from 60 up to 350 m^2/g were obtained.

Temperature programmed desorption of pyridine was applied to characterize the zeolite acidity. A decrease of the number of Brönsted acid sites with a higher F/Si ratio in the starting synthesis solution was observed. Based on the Hammett acidity function H_0, a model has been developed to correlate the Brönsted acidity of the resulting zeolitic material with the amount of fluoride anions introduced. Thus, ZSM-5 zeolites with tailored properties both at the molecular and microscopic levels are obtained.

Keywords: ZSM-5; Zeolite; Fluoride anions; Hammet acidity; H_0; Structured catalytic materials

1. Introduction

ZSM-5 zeolites are well-known crystalline microporous aluminosilicates that possess three-dimensional frameworks [1,2]. Aluminum atoms in the framework introduce negative charges, which are counter-balanced by extra-framework cations. If such cations are hydrogen ions then the zeolite is a solid exhibiting Brönsted acidity. Hydrothermal treatment results in dealumination with *extra*-framework Al possessing Lewis acidity. Moreover, the pores of zeolites have uniform sizes comparable to molecular dimensions introducing molecular sieve functions.

ZSM-5 is one the most studied zeolites due to its application in many fields like separation of gases or liquids [3,4], synthesis of fine chemicals [5,6], the one-step phenol production [5,7,8], in space research [9], and essentially as a solid acid catalyst [10–12]. In order to extend the catalytic applications, the new synthesis routes of ZSM-5 with controlled morphology, pore architecture and surface acidity are warranted.

A significant breakthrough in the field of zeolite synthesis occurred when hydroxyl anions were replaced by fluorides, making the synthesis possible in neutral and even in acidic media (pH = 5) [13]. Later on, Guth and Kessler developed the synthesis of several microporous materials: aluminosilicates, aluminophosphates, gallophosphates via this alternative non-alkaline route [14–18]. The use of the fluoride ion as mineralizer (by using NH_4F source) instead of the conventionally used hydroxide ion presents several advantages:

* Corresponding author. Present address: Laboratoire des Matériaux, Surfaces et Procédés pour la Catalyse (LMSPC), ECPM, Université Louis Pasteur, 25 rue Becquerel, 67087 Strasbourg Cedex 02, France. Tel.: +33 390242675; fax: +33 390242674.
E-mail address: blouis@chimie.u-strasbg.fr (B. Louis).

1387-1811/$ - see front matter © 2004 Elsevier Inc. All rights reserved.
doi:10.1016/j.micromeso.2004.06.016

- fewer metastable phases are formed, which implies a certain ease of preparation of any desired zeolite [17,19,20],
- synthesis of materials not obtainable in alkaline media like the 20-T-ring gallophosphate cloverite [21],
- formation of large crystals with few defects which are of interest as model host materials (for adsorption or diffusion studies) [22],
- neutral medium (or acidic) enables the incorporation of elements sparingly soluble in alkaline media: Co^{2+}, Fe^{3+}, Ti^{4+} [16,17],
- direct formation of the ammonium form NH_4–ZSM-5, instead of Na–ZSM-5 avoiding repeated ion-exchange; so only a calcination step is needed to burn off the template and to obtain the acidic H–ZSM-5.

Recent studies have shown that even after calcination fluorine remains occluded inside the small $[4^15^26^2]$ cages found in the MFI structure [19,23,24]. In spite of the numerous advantages of the synthesis in fluoride media, the presence of such highly electronegative element modifies the electron density around the neighbouring Si by the formation of $[SiO_{4/2}F]^-$ entities [23–25]. Thus, this may also influence the catalytic properties of the zeolite.

This study deals with the synthesis of H–[F]ZSM-5 zeolites with different F/Si ratio in order to investigate the effect of fluorine on the physico-chemical properties of the materials: degree of crystallinity, specific surface area (SSA), size of the crystals, and also the zeolite acidity. The aim is to tailor both chemical and morphological microscopic properties. Furthermore, industry continuously requires new structured catalyst packings [3,26]. In reactors containing such packings, the pressure drop, the flow characteristics, the mass and heat transfers are found to be improved if compared to randomly packed catalytic beds. Our previous studies reported the in situ growth of ZSM-5 crystals on well-arranged macroscopic supports (metals or ceramics) [8,27,28].

So, the work is aimed on the understanding of the triple-scale design of zeolite materials from the regulation of surface acidity (molecular scale), defined crystal size and morphology (microscopic level) up to the reactor with structured catalytic bed (macro-scale).

2. Experimental

2.1. Synthesis of H–[F]ZSM-5 materials

The synthesis mixture was prepared by adding to demineralised water at room temperature: sodium aluminate (52.5 wt% $NaAlO_2$, Riedel-de-Haën), tetrapropylammonium bromide (TPA-Br, 99%, Merck-Suchardt), and ammonium fluoride (NH_4F, >98%, Fluka). Then, tetraethyl orthosilicate (TEOS, 98%, Merck-Suchardt) was introduced under vigorous stirring. The mole ratios were as follows: TPA-Br:TEOS: $NaAlO_2$:NH_4F:H_2O = 0.07:1:0.012:0.3–1.6:80. The pH was adjusted to 7 by adding a few drops of hydrofluoric acid solution (40 wt%).

The mixture was homogenised and aged for 3 h. The gel was then poured into an autoclave and maintained for 135 h at 443 K. The crystalline material was filtered, washed with demineralised water and dried at 393 K. The H-forms were obtained by 5 h calcination at 773 K in air.

For comparison a synthesis in alkaline media was performed. The mole ratios were as follows: TPA-OH: TEOS:NaCl:$NaAlO_2$:H_2O = 2.2:5.6:3.4:0.13:1000. The mixture was homogenised and allowed to age during a time of 3 h. Similar synthesis conditions (time, temperature, pressure) were used to produce both [F]–ZSM-5 and non-fluorinated materials.

The yield of the synthesis was defined as the ratio of silicon incorporated into the zeolite matrix to the initial amount of silicon in the synthetic mixture.

2.2. Characterisation

The specific surface areas (SSA) and the porosity of the zeolites were measured by nitrogen adsorption–desorption at 77 K with a Sorptomatic 1900 instrument (Carlo–Erba). Prior to the measurements, the samples were heated for 2 h in vacuum to 523 K. The SSA (internal + external surfaces) were determined by the BET method.

The X-ray diffraction (XRD) spectra were acquired on a D500 Siemens powder diffractometer ($\theta/2\theta$) using monochromatised Cu-$K_{\alpha 1}$ radiation (λ = 1.5406 Å) in the range of 2θ from 5° to 50° with a step of 0.04° every 8 s.

XRD was used to validate the synthesis procedure, in respect to the crystalline structure comparing the patterns obtained with the JCPDS tables. Afterwards the degree of crystallinity (Q) was determined. It was calculated as the sum of the seven highest reflections in the XRD pattern [29] referred to this sum of the most crystalline sample with F/Si = 1.1, which degree of crystallinity was set to Q = 1.

The XPS study was performed to determine the chemical composition of the surfaces. The measurements were carried out via a PHI-550 ESCA system (Perkin–Elmer) with energy variation between 0 and 1100 eV using K_α radiation of Mg.

Scanning electron microscopy (SEM) was employed to study the morphology of the zeolite crystals. The SEM images were recorded with a JEOL JSM-6300F electron microscope operated at a voltage of 5 kV. The Si/Al ratio of the crystals was determined by energy-dispersive X-ray (EDAX) analysis in the SEM chamber.

The temperature programmed desorption (TPD) of pyridine was used to titrate the different types of acid sites (Lewis and Brönsted) of the zeolites in order to evaluate their acid–base properties. The measurements were performed in a Micromeritics AutoChem 2910 analyser provided with a quartz plug-flow reactor. A ThermoStar 200 (Pfeiffer Vacuum) mass-spectrometer was used to analyse the gas-phase composition. It was calibrated by gas-chromatography using mixtures of known composition. The catalysts were pre-treated by heating at 823 K in He for 2 h.

The pyridine-containing mixture (~3 vol.% in He) was obtained by saturation at room temperature in a bubble column with anhydrous pyridine (>99.8%, Fluka) and was introduced into the reactor with a sample (30 mg) at 473 K until adsorption equilibrium was attained. After purging with He for 5 min a TPD was started with the temperature ramp of 10 K/min up to 1173 K in a He flow of 20 ml STP/min. The outlet gas stream was monitored for H_2O (18 m/e), CO_2 (44 m/e) and pyridine (52 and 72 m/e).

3. Results and discussion

3.1. Elemental analysis and BET

The synthesis yields for all samples were about 71 ± 5%.

The Si/Al ratio of the zeolite prepared with a ratio F/Si = 1.6 was found to be 41. Moreover, the chemical composition of this sample was also analysed by XPS (Fig. 1). The presence of Al (signal at 70 eV) confirms that ZSM-5 was obtained, rather than silicalite-1. Fluorine has also been detected (690 eV) after the template removal. Its atomic composition was estimated to be 1.6 wt%. This indicates that F^- anions are not only present as a charge-balancing ion of the organic template, but retained inside the zeolite channels. Recent studies [19,23,24] have undoubtedly shown that even after template removal, fluorine stays inside the small $[4^15^26^2]$ cages found in the MFI structure.

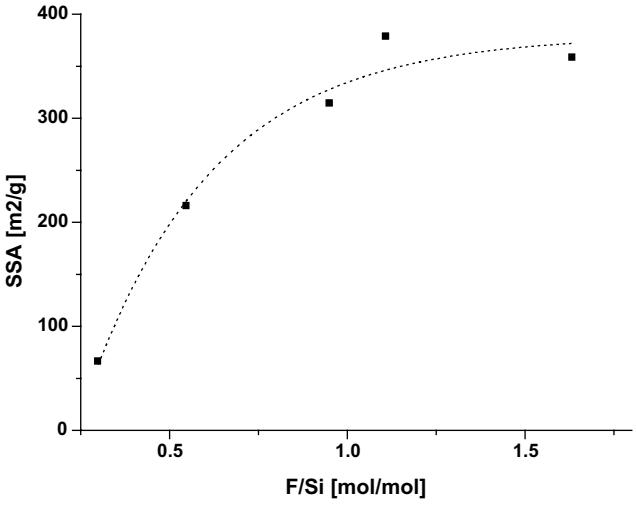

Fig. 2. Specific surface areas as a function of the F/Si ratio.

Fig. 2 presents the plot of the SSA values against the F/Si ratio. It appears that the SSA values are related to the amount of fluoride introduced into the synthesis mixture and can be varied from 60 up to 350 m^2/g. The total pore volume of the fluorinated materials was about 0.27 cm^3/g, which is in line with the literature data [30].

3.2. Powder X-ray diffraction and SEM studies

Fig. 3 presents an XRD pattern of H–[F]ZSM-5 (F/Si = 1.1) showing the characteristics of the MFI

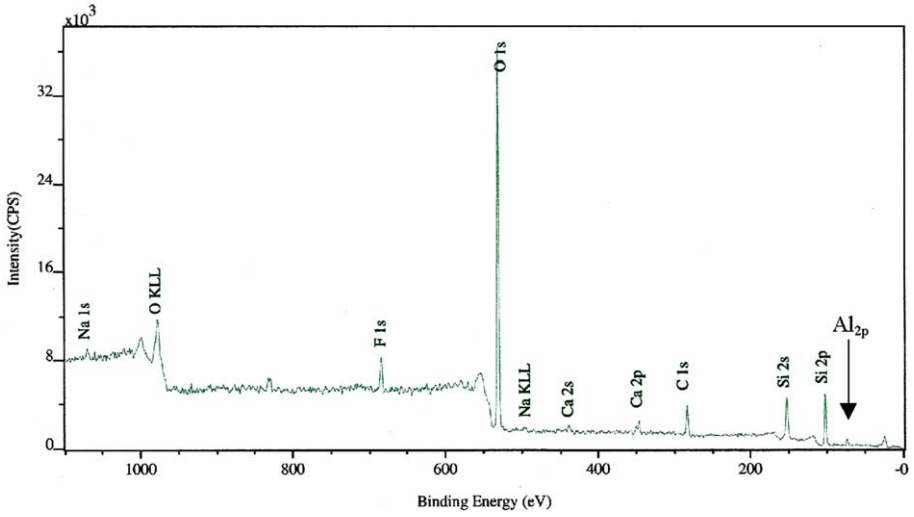

Fig. 1. XPS spectra of calcined H–[F]ZSM-5 (F/Si = 1.6) zeolite.

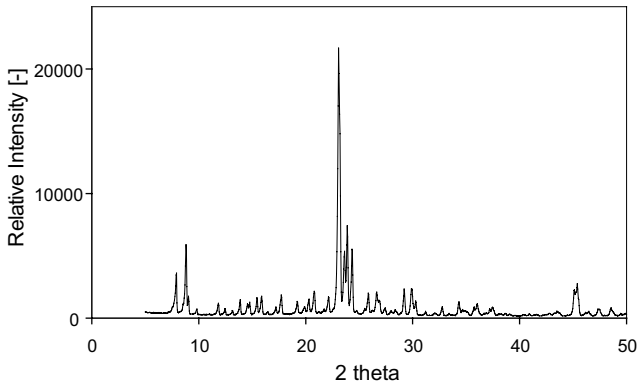

Fig. 3. XRD pattern of H–[F]ZSM-5 (F/Si = 1.1).

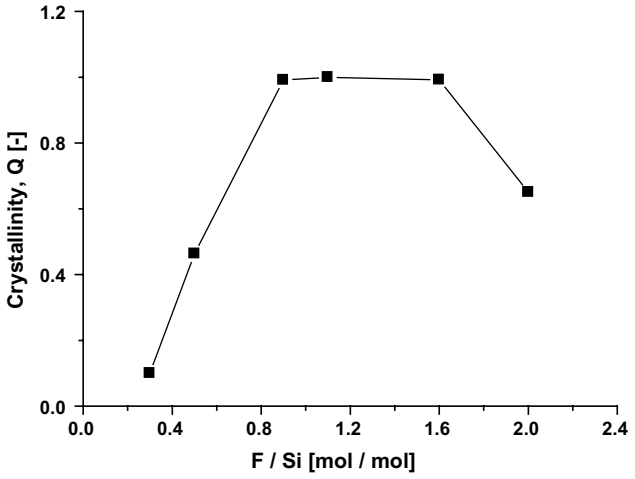

Fig. 4. Degree of crystallinity as a function of the F/Si ratio.

structure [2,31]. This sample was found to be the most crystalline and therefore its degree of crystallinity (Q) was set to unity.

Fig. 4 shows the degree of crystallinity as a function of the F/Si ratio. It can be seen that the Q values are close to unity for the samples with F/Si ratio 0.9–1.6. At lower and higher fluoride concentrations (F/Si = 2) the zeolites are only partially crystalline. The dependence of the crystallinity on the F/Si ratio has the same trend as the SSA (see Fig. 2). This suggests that the structural parameters of the zeolites are related to the amount of fluoride introduced in the synthesis mixture. This follows the observations made by Corma and coworkers who reported that fluoride ions may catalyse the condensation reaction involved in Si–O–Si bond formation [42].

The size of the crystals is found to be dependent on the fluoride concentration (Fig. 5a–d). The typical prismatic morphology of the ZSM-5 crystals is seen in the SEM micrographs. Fig. 5a confirms the presence of amorphous material for F/Si = 0.3–0.5. The crystals obtained with fluoride are larger than those produced by the synthesis in alkaline media, where a size of about 5 μm was observed [28].

Furthermore, their crystallinity is also about 20% higher. Because of the superior quality of the products, there is considerable interest in understanding the role that the fluoride anions play in the synthesis of zeolites under these conditions. The replacement of OH^- by F^- ions as mineraliser appears to be a prerequisite for the formation of both large and well-crystallised crystals.

Table 1 summarises the data obtained by XRD and SEM studies. It is seen that a higher concentration of F^- in the synthesis solution leads to the formation of larger crystals. It can be concluded that the syntheses via this unconventional route allows to vary the size of the crystals maintaining high crystallinity $Q = 1$. Since a part of the F^- ions remain in the zeolite structure after the template removal, the chemical properties and thus the catalytic behaviour can be affected [23,24].

3.3. Acid–Base properties: Brönsted acid sites titration

The acid–base surface properties of the fluorinated zeolites were investigated via TPD of pyridine. The chemisorption of pyridine allows to distinguish between Brönsted acid sites (one pyridine molecule forming one pyridinium ion, PyH^+) and Lewis acid sites (binds pyridine coordinately, PyL).

Fig. 6a shows the TPD profile obtained on the ZSM-5 with the F/Si = 1.6. The pyridine desorption takes place without decomposition and apparently occurs from two types of sites. The desorption from the first site corresponds to the peak between 250 and 330 °C, while the second site is responsible for the peak between 530 and 580 °C. The peak below 330 °C (LT) is assigned to the pyridine coordinated on Lewis sites (PyL) and on non-acidic silanol groups [32]. The high-temperature desorption peak (HT) is assigned to the strongly adsorbed pyridine on Brönsted acid sites [33]. The H–[F]–ZSM-5 sample was also exchanged several times in a $NaCH_3O$ solution in THF [34]. The HT peak was not observed in the spectra, indicating a loss of the Brönsted acid sites (see Fig. 6b). This confirms the previous assumption that the HT peak is assigned to the adsorption of pyridine on Brönsted acid sites. Furthermore, for H-MFI samples, one molecule of pyridine adsorbs on one OH site forming 1:1 complexes [35]. Therefore, the amount of the Brönsted acid sites can be determined by measuring the adsorbed pyridine on the OH groups (HT peak in the TPD profile).

Fig. 7 presents the dependence of the number of Brönsted acid sites of the crystalline H–[F]ZSM-5 samples (F/Si = 0.9, 1.1, and 1.6) on the F/Si ratio. For comparison, a zeolite was synthesised under alkaline conditions in the same manner as the fluorinated materials, transformed to the H-form via three-time

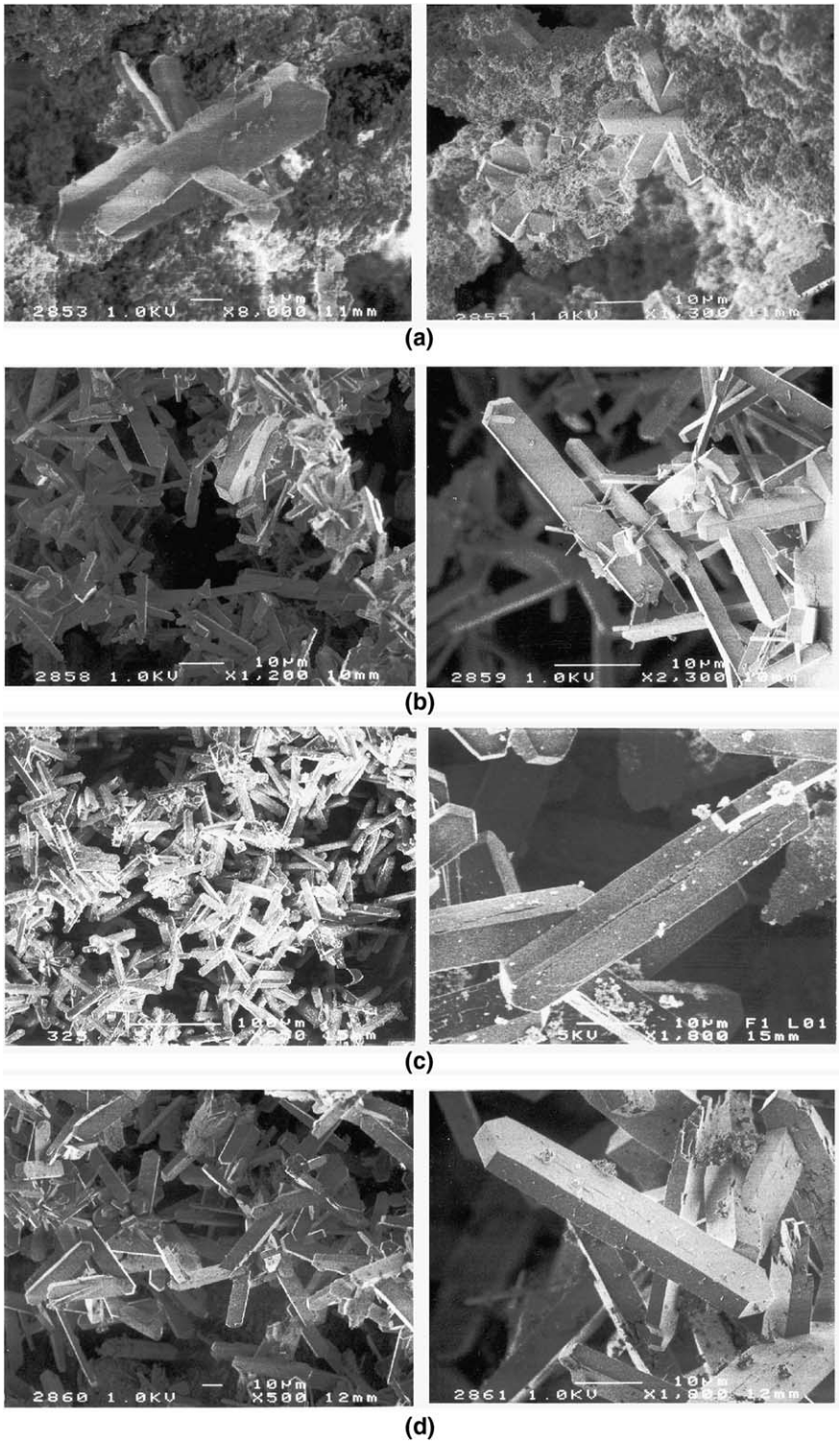

Fig. 5. SEM micrographs of fluorinated materials: (a) F/Si = 0.3 (left); F/Si = 0.5 (right); (b) F/Si = 0.9; (c) F/Si = 1.1; (d) F/Si = 1.6.

exchange with ammonium chloride [34] followed by calcination in air for 5 h at 773 K. It is noteworthy that an increase of the concentration of fluorides in the synthesis gel tends to decrease the number of Brönsted acid sites in the resulting material.

For the zeolite sample with F/Si = 1.6, and having a Si/Al = 41, the theoretical amount of Brönsted acid sites should be about 0.4 mmol H^+/g. The measured value for the sample having a F/Si = 1.6 is about 0.05 mmol $H^+/g_{zeolite}$. Therefore, the fluoride anions really present

Table 1
Degree of crystallinity and size of the crystals in different samples

Sample F/Si	Degree of crystallinity Q (–)	Size of the crystals (μm)
0.3	~0.1	$10.2 \times 2.1 \times 0.6$
0.5	0.463	$34.5 \times 7.5 \times 2.7$
0.9	0.991	$18.3 \times 7.5 \times 2.9$
1.1	1	$54.0 \times 8.1 \times 5.4$
1.6	0.992	$76.3 \times 13.8 \times 10.0$

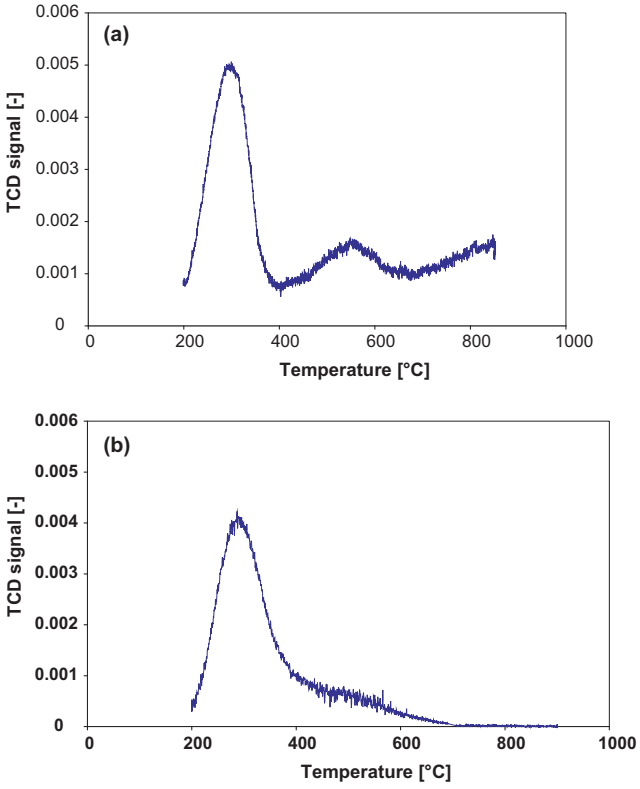

Fig. 6. TPD of pyridine from the (a) fluorinated zeolite with F/Si = 1.6, (b) [Na]-back-exchanged fluorinated sample F/Si = 1.6.

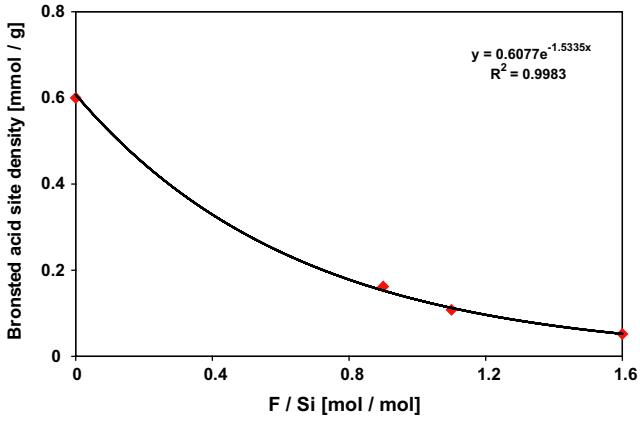

Fig. 7. Surface concentration of Brönsted acid sites as a function of the F/Si ratio.

an effect on the total amount of Brönsted acid sites. Harris and coworkers [36] have shown that the presence of fluoride ions can complex aluminum atoms and form AlFx species (shown by REDOR NMR techniques), thus avoiding the formation of Brönsted acid sites. Therefore, it appears to some extend that the presence of fluoride anions tend to decrease the incorporation of aluminum inside the zeolite framework.

Moreover, the HT desorption peak is also shifted toward lower values while increasing the fluorine content: from 611 °C for the sample having a F/Si = 0.9 to 550 °C for the sample with F/Si = 1.6. The sample synthesised in the presence of an alkali media presents a HT peak with a maximum at 633 °C.

It follows that both the number of Brönsted sites and also their strength are reduced while increasing the concentration of fluorides in the gel.

4. Modelling of zeolite acidity by the Hammett acidity function H_0

The difference in the acidity strength of the zeolite with F^- inside cavities can be due to the electron inductive effect (acceptor character of F^- anions), where F atoms could accept electronic density from the neighbouring Si, decreasing the Si–O bond length, thus decreasing the lability of the proton [23,37]. Since Brönsted acid sites act as counter ions for $[SiO_{4/2}F]^-$ entities [23–25], their lability, and thus their acidity is decreased. Fig. 7 shows the exponential dependence of the number of Brönsted acid sites on the F/Si ratio. So, it can be represented by Eq. (1), or in linear form by Eq. (2):

$$[H^+] = A \cdot e^{-B[F^-]} \tag{1}$$

$$\ln[H^+] = \ln A - B[F^-] \tag{2}$$

So, after linearization of Eq. (1), the proportionality between the logarithm of the concentration of Brönsted acid sites and the concentration of F^- anions is obtained. By replacing the natural logarithm by the logarithm in base 10, one comes to Eq. (3):

$$-\log_{10}[H^+] = -\log_{10} A + B[F^-]/\ln 10 \tag{3}$$

The decrease observed in the Brönsted acidity with a higher concentration of fluorides in the zeolite can be based on the Hammett acidity function H_0 as described in Eq. (4):

$$\mathrm{pH} = -\log_{10} A + B[F^-]/\ln 10 \iff H_0 = -\log_{10} A + B[F^-]/\ln 10 \tag{4}$$

Hammett's principle claims that the concentration of $[H^+]$ cannot satisfactorily characterise the acidity due to the $[H^+]$ solvated diversely. Therefore, the ability of proton transfer to a base depends on the nature of the med-

ium [38]. Hammett and Deyrup were the first to suggest a method for measuring the degree of protonation of weak bases in acid solutions [39]. In dilute aqueous solutions, as the activity coefficients tend to unity, the Hammett acidity function H_0 becomes identical with pH.

Therefore, the last equation (Eq. (4)) presents the equivalence between the pH scale used in liquid media and the Hammett acidity function H_0 used in strong acid media. This assumption is confirmed by the fact that Hammett explored the whole H_2O–H_2SO_4 range up to 100% sulphuric acid, and Haw and coworkers estimated the HZSM-5 acidity to about 70% H_2SO_4 [40]. Furthermore, Rys and Steinegger have developed a model relating the sorption of bases in acid solids with the sorption of the same bases in acid solution [41]. Their results showed that Hammett's postulate, i.e. that bases with similar structure have similar activity coefficients in homogeneous acid solutions also holds within the pore structure of solid acids [41].

So, the acid strength of the fluorinated materials (expressed in decreasing values for H_0) appears to be proportional to a decrease of $[F^-]$ values, which is in line with our experimental results. The presence of fluorine inside the zeolite after calcination can be the reason for such linear dependence between the acidity and the concentration of F^-.

The resulting relationship (Eq. (4)) from this model, allows an estimation of the acidity function H_0 of these fluorinated zeolites.

Depending on application requirements, one should be able to tailor the acidity of MFI zeolites by varying the concentration of F^-. Moreover, this should allow the controlling of the chemical properties with an appropriate and defined crystal size. This synthesis strategy can be employed to prepare less acidic ZSM-5 zeolites, having relatively large and well-defined crystals (>10 μm). Nevertheless, this work shows that the acidity, the crystallinity and the particle size are not independent variables. So, it would be difficult to prepare a very acidic zeolite having a large crystal size.

Fortunately, the triple-scale design is possible, if these molecular and microscopic properties are conjugated with an appropriate macroscopic characteristics of structured reactors [8,27].

5. Conclusions

H–[F]ZSM-5 zeolites with high crystallinity and high specific surface area were synthesised and characterised by physico-chemical techniques. By varying the concentration of fluorides in the gel, it is possible to tailor the size of the crystals and their surface acidity.

An exponential dependence between the number of Brönsted acid sites on the zeolite surface and the concentration of fluorides was observed. A model was proposed to characterize the zeolite acidity by the Hammett acidity function H_0.

Innovative structured zeolitic materials can be produced via a fine tuning of the molecular, micro- and macroscopic properties.

Acknowledgments

Financial support from the Swiss National Foundation is gratefully acknowledged. The authors highly appreciated fruitful discussions with Prof. A. Renken and clever advices of Mr. F. Rainone. We also thank Mrs. N. Marti, M.E. Casali, B. Senior, N. Xanthopoulos, and I. Stolitchnov for the technical assistance.

References

[1] R.J. Argauer, G.R. Landolt, US 3,702,886, United States, 1969.
[2] C. Baerlocher, W.M. Meier, D.H. Olson, Atlas of zeolite framework types, fifth ed., Elsevier, Amsterdam, 2001.
[3] H. van Bekkum, E.R. Geus, H.W. Kouwenhoven, Stud. Surf. Sci. Catal. 85 (1994) 509.
[4] A. Dyer, An introduction to zeolite molecular sieves, John Wiley & sons, New York, 1988.
[5] W.F. Hölderich, H. van Bekkum, Stud. Surf. Sci. Catal. 58 (1991) 631.
[6] A. Corma, H. Garcia, Catal. Today 38 (1997) 257.
[7] M. Häfele, A. Reitzmann, D. Roppelt, G. Emig, Appl. Catal. A 150 (1997) 153.
[8] B. Louis, L. Kiwi-Minsker, P. Reuse, A. Renken, Ind. Eng. Chem. Res. 40 (2001) 1454.
[9] H. Ghobarkar, O. Schäf, U. Guth, Prog. Solid State Chem. 27 (1999) 29.
[10] N.Y. Chen, Ind. Eng. Chem. Res. 40 (2001) 4157.
[11] A. Corma, Chem. Rev. 95 (1995) 559.
[12] C.J.A. Mota, P.M. Esteves, A. Ramirez-Solis, R. Hernandez-Lamoneda, J. Am. Chem. Soc. 119 (1997) 5193.
[13] E.M. Flanigen, R.L. Patton, US 4,073,865, United States, 1978.
[14] H. Kessler, J. Patarin, C. Schott-Darie, Stud. Surf. Sci. Catal. 85 (1994) 75.
[15] J.L. Guth, H. Kessler, M. Bourgogne, Fr 2564451, France, 1984.
[16] J.L. Guth, P. Caullet, J. Chim. Phys. 83 (1986) 155.
[17] J.L. Guth, H. Kessler, J.M. Higel, J.M. Lamblin, J. Patarin, A. Seive, J.M. Chezeau, R. Wey, Zeolite synthesis, in: ACS Symp. Ser. 398, Washington DC, 1989, p. 176.
[18] J.L. Guth, L. Delmotte, M. Soulard, N. Brunard, J.F. Joly, D. Espinat, Zeolites 12 (1992) 929.
[19] M.A. Camblor, L.A. Villaescusa, M.J. Diaz-Cabanas, Topic Catal. 9 (1999) 59.
[20] S.A. Axon, J. Klinowski, J. Chem. Soc. Faraday Trans. 86 (1990) 3679.
[21] M. Estermann, L.B. McCusker, C. Baerlocher, A. Merrouche, H. Kessler, Nature 352 (1991) 320.
[22] F. Schüth, W. Schmidt, Adv. Mater. 14 (2002) 629.
[23] A.R. George, C.R.A. Catlow, Chem. Phys. Lett. 247 (1995) 408.
[24] C.A. Fyfe, D.H. Brouwer, A.R. Lewis, J.M. Chezeau, J. Am. Chem. Soc. 123 (2001) 6882.
[25] H. Koller, A. Wölker, H. Eckert, C. Panz, P. Behrens, Angew. Chem. Int. Ed. Eng. 36 (1997) 2823.
[26] A. Cybulski, J.A. Moulijn, The present and future of structured catalysts—an overview, Marcel Dekker, New York, 1998.

[27] B. Louis, C. Tezel, L. Kiwi-Minsker, A. Renken, Catal. Today 69 (2001) 365.
[28] B. Louis, P. Reuse, L. Kiwi-Minsker, A. Renken, Appl. Catal. A 210 (2001) 103.
[29] S.A. Axon, J. Klinowski, Appl. Catal. 56 (1989) 9.
[30] M. Müller, G. Harvey, R. Prins, Micropor. Mesopor. Mater. 34 (2000) 135.
[31] G.L. Woolery, G.H. Kuehl, H.C. Timken, A.W. Chester, J.C. Vartuli, Zeolites 19 (1997) 288.
[32] D.J. Parillo, A.T. Adamo, G.T. Kokotailo, R.J. Gorte, Appl. Catal. 67 (1990) 107.
[33] L.J. Lobree, I.C. Hwang, J.A. Reimer, A.T. Bell, J. Catal. 186 (1999) 242.
[34] B. Louis, Synthesis of ZSM-5 coatings on metals and glass–fibres: an effective structured catalyst for the partial oxidation of benzene by N_2O, PhD Thesis 2651, Ecole Polytechnique Federale de Lausanne, EPFL, Lausanne, 2002.
[35] R.J. Gorte, Catal. Lett. 62 (1999) 1.
[36] R.D. Gougeon, E.B. Brouwer, P.R. Bodart, L. Delmotte, C. Marichal, J.M. Chezeau, R.K. Harris, J. Phys. Chem. B 105 (2001) 12249.
[37] A.R. George, C.R.A. Catlow, Zeolites 18 (1997) 67.
[38] G.A. Olah, G.K.S. Prakash, J. Sommer, Superacids, John Wiley and Sons, New York, 1985.
[39] L.P. Hammett, A.J. Deyrup, J. Am. Chem. Soc. 54 (1932) 2721.
[40] T. Xu, E.J. Munson, J.F. Haw, J. Am. Chem. Soc. 116 (1994) 1962.
[41] P. Rys, W.J. Steinegger, J. Am. Chem. Soc. 101 (1979) 4801.
[42] P.A. Barrett, M.A. Camblor, A. Corma, R.H. Jones, L.A. Villaescusa, J. Phys. Chem. B. 102 (1998) 4147.